doi:10.1111/j.1558-5646.2007.00158.x

ANTAGONISTIC COEVOLUTION MEDIATED BY PHENOTYPIC DIFFERENCES BETWEEN QUANTITATIVE TRAITS

Scott L. Nuismer,[1,2] Benjamin J. Ridenhour,[1] and Benjamin P. Oswald[1]

[1] *Department of Biology, University of Idaho, Moscow, Idaho 83844*

[2] *E-mail: snuismer@uidaho.edu*

Received September 19, 2006
Accepted March 19, 2007

Many well-studied coevolutionary interactions between predators and prey or hosts and parasites are mediated by quantitative traits. In some interactions, such as those between cuckoos and their hosts, interactions are mediated by the degree of phenotype matching among species, and a significant body of theory has been developed to predict the coevolutionary dynamics and outcomes of such interactions. In a large number of other cases, however, interactions are mediated by the extent to which the phenotype of one species exceeds that of the other. For these cases—which are arguably more numerous—few theoretical predictions exist for coevolutionary dynamics and outcomes. Here we develop and analyze mathematical models of interspecific interactions mediated by the extent to which the quantitative trait of one species exceeds that of the other. Our results identify important differences from previously studied models based on trait matching. First, our results show that cyclical dynamics are possible only if the strength of coevolutionary selection exceeds a threshold and stabilizing selection acts on the interacting traits. Second, our results demonstrate that significant levels of genetic polymorphism can be maintained only when cyclical dynamics occur. This result leads to the unexpected prediction that maintenance of genetic polymorphism is enhanced by strong selection. Finally, our results demonstrate that there is no a priori reason to expect the traits of interacting species should match in any literal sense, even in the absence of gene flow among populations.

KEY WORDS: **Coevolutionary hotspots, escalation, geographic mosaic, host-parasite, matching, predator-prey.**

Many coevolutionary interactions are mediated by quantitative traits. Well-studied examples include interactions between newts and their garter snake predators (Brodie and Brodie Jr. 1999; Brodie et al. 2002), wild parsnip and their parasitic webworms (Berenbaum et al. 1986; Berenbaum and Zangerl 1992), pines and seed-predatory crossbills (Benkman 1999, 2003), and parasitic cuckoos and their avian hosts (Davies and Brooke 1989; Soler et al. 2003). Recent empirical research on these systems has identified intriguing spatial patterns, such as variation in the degree of phenotype matching between the interacting species (Zangerl and Berenbaum 2003), variation in the extent to which defenses and counter defenses are exaggerated (Geffeney et al. 2005), and variation in the success of parasitism (Soler et al. 1999).

It has been suggested for these systems—as well as many others—that the observed spatial patterns result from the interplay between coevolutionary hotspots and coldspots, selection mosaics, and trait remixing (e.g., gene flow) as envisioned by Thompson's geographic mosaic theory (Benkman 1999; Soler et al. 2001; Brodie et al. 2002; Zangerl and Berenbaum 2003; Thompson 2005). Evaluating the validity of this suggestion is made difficult, however, by the absence of a well-developed theoretical framework for coevolutionary interactions mediated by quantitative traits. Consequently, it is currently impossible to discern whether a geographic mosaic process is required to explain existing empirical results (Benkman 1999; Soler et al. 2001; Brodie et al. 2002; Zangerl and Berenbaum

2003; Toju and Sota 2006), or whether these results can be adequately explained by simpler models of single isolated communities.

Existing theory developed for coevolutionary interactions mediated by quantitative traits has primarily focused on those interactions that depend on the degree of trait "matching" between species (e.g., Dieckmann et al. 1995; Gavrilets 1997; Nuismer et al. 2005; Kopp and Gavrilets 2006). For instance, the probability that the egg of a parasitic cuckoo is rejected by the host depends on the similarity of host and parasite egg morphologies (Robert and Sorci 1999). Several other well-studied systems depend on the extent of phenotype matching among species as well (e.g., Benkman 1999, 2003; Clayton et al. 2003). Recent genetically explicit models have shown that these interactions generally produce cyclical dynamics in which the degree of phenotype matching fluctuates over time (Nuismer et al. 2005). In some cases, however, equilibria can be reached where the degree of phenotype matching depends on the relative strengths of stabilizing and coevolutionary selection (Gavrilets 1997; Kopp and Gavrilets 2006). Consequently—for interactions mediated by phenotype matching between species—spatial variation in the extent of trait matching, the efficacy of parasitism, or exaggeration of traits can be explained without recourse to a geographic mosaic process that explicitly invokes a role for "trait remixing" (Gomulkiewicz et al. 2007).

Although many coevolutionary interactions are described by a mechanism of phenotype matching, many others depend on the extent to which the trait value of one species exceeds that of the other. For instance, in interactions between parsnip web-worms and wild parsnip, those web-worms with a greater concentration of the detoxifying enzyme P450 are better able to feed on wild parsnip plants protected by toxic furanocoumarins (Berenbaum et al. 1986; Berenbaum and Zangerl 1992). Many other well-studied coevolutionary interactions are mediated in a similar fashion (e.g., Bergelson et al. 2001; Brodie et al. 2002; Toju and Sota 2006), and for some broad classes of interactions, such as those between plants and insect parasites, this may be the dominant form of interaction between quantitative traits (Bergelson et al. 2001). In contrast to those interactions that depend on the degree of phenotype matching, little theory has been developed for this case, and what theory has been developed generally focuses on the consequences of coevolution for demographic dynamics in systems with relatively simple genetic underpinnings (e.g., Saloniemi 1993; Abrams 2000; Nuismer and Kirkpatrick 2003). Consequently, there are few genetically robust predictions for the coevolutionary dynamics and outcomes of these interactions even for only single, spatially isolated communities.

Here we address this gap in existing theory by developing a model of coevolution in which the outcome of the interaction depends on the extent to which the trait value of one species exceeds that of the other. We analyze this model in three ways. First, we assume selection is weak and genetic variance is fixed allowing us to develop analytical solutions. Second, we relax the assumption of fixed genetic variance and analyze the model using a quasi-linkage equilibrium (QLE) approximation that assumes weak selection and frequent recombination. Finally, we use numerical simulations to consider cases in which genetic variance can evolve and selection is strong. Our goal with these analyses is to develop robust expectations for the conditions that give rise to various classes of coevolutionary dynamics and outcomes in the absence of explicit spatial structure. We then evaluate the extent to which our model of a single geographically isolated community can explain the spatial variation in defensive and counter defensive traits observed in several well-studied coevolutionary interactions.

The Model

We modeled coevolution between a pair of species that interact antagonistically. For simplicity, we use the words parasite and host throughout our description, but the same model could apply to coevolution between a predator and prey or herbivore and food plant. Each species is assumed to mate at random, encounter individuals of interacting species at random, and have a population size sufficiently large for the effects of genetic drift to be negligible. In addition, we assume an individual's fitness is independent of population sizes and thus ignore potentially important feedbacks between demography and selection (e.g., Burdon and Thrall 1999, 2000; Abrams 2000; Benkman et al. 2001).

We assume interspecific interactions are mediated by a single trait in each species. The probability of a successful parasite attack increases as the value of the parasite trait (z_P) increases relative to the host trait (z_H) (Fig. 1). We modeled this scenario by assuming the probability of a successful parasite attack is

$$P_A = 1/(1 + \exp[-\alpha(z_P - z_H)]), \quad (1)$$

where α measures how sensitive the probability of a successful parasite attack is to the difference in host and parasite phenotype. An attack function of this form has been shown to be important in interactions between parasites and toxic host plants (Bergelson et al. 2001), seed parasites and host plants (Toju and Sota 2006), and toxic newts and their garter snake predators (Brodie and Ridenhour 2003). The analytical approaches described in detail below make use of an approximation to (1) that assumes the probability of a successful parasite attack varies only weakly over the range of host and parasite phenotypes (e.g., Fig. 1A).

Because traits mediating species interactions are also likely to be subject to constraints imposed by physiology or the abiotic environment (Fellowes et al. 1998; Brodie and Brodie Jr. 1999; Webster and Woolhouse 1999; Bergelson et al. 2001; Lahti 2005),

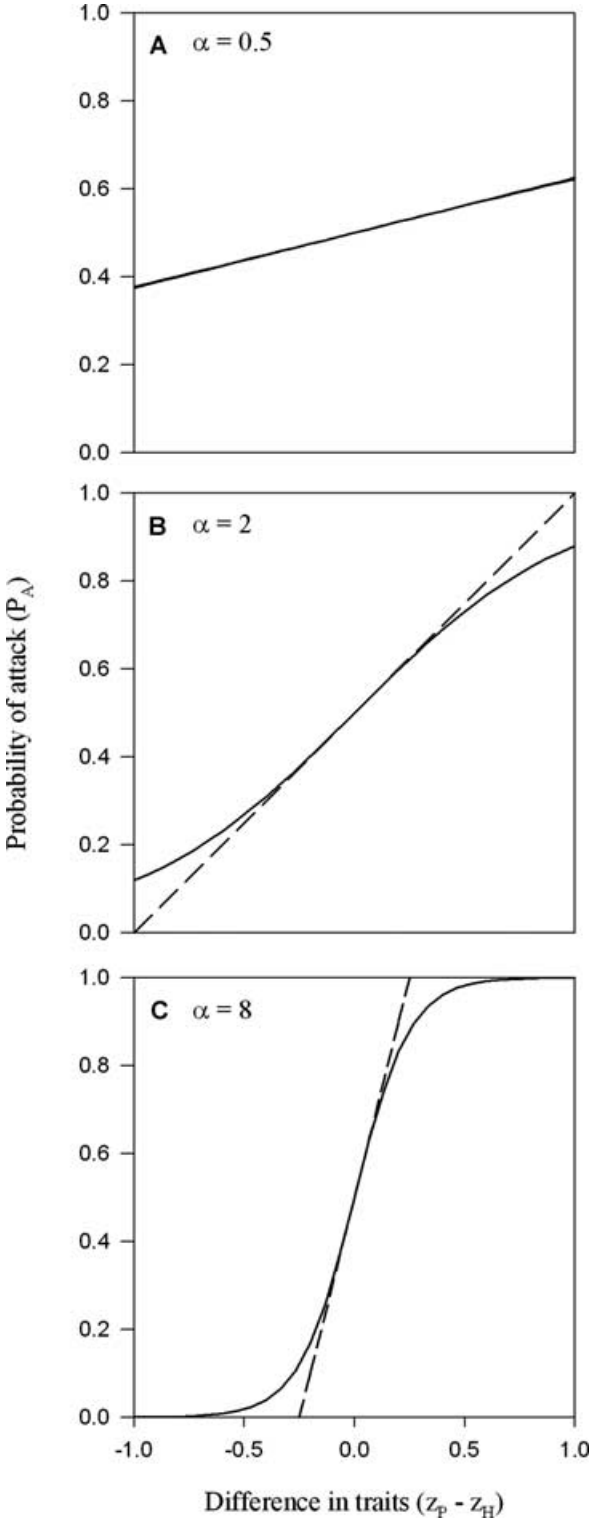

Figure 1. The probability of a successful parasite attack (P_A) as a function of host and parasite phenotypes for three values of the parameter α. The solid line in each panel is drawn from equation (1) and is thus exact. In contrast, the dashed line is drawn from a first-order Taylor Series approximation to (1), which assumes α is small. This approximation yielded the formula $P_A = 1/2 + \alpha/4(z_P - z_H)$. Values of α were: (A)$\alpha = 0.5$, (B) $\alpha = 2.0$, and (C)$\alpha = 8.0$.

we allow stabilizing selection to act on the traits (z_H, z_P) of the interacting species. With these assumptions, the fitness of a host individual with phenotype z_H in an encounter with a parasite individual with phenotype z_P is

$$W_H(z_H, z_P) = \exp[-\gamma_H(z_H - \theta_H)^2](1 - \xi_H P_A), \quad (2)$$

where γ_H is the strength of stabilizing selection acting on the host trait, and measures the sensitivity of an individual's fitness to its phenotypic distance from a static optimal value, θ_H. The parameter ξ_H measures the fitness cost imposed on the host by a successful parasite attack. Similarly, the fitness of a parasite individual with phenotype z_P in an encounter with a host individual with phenotype z_H is

$$W_P(z_P, z_H) = \exp[-\gamma_P(z_P - \theta_P)^2](1 - \xi_P(1 - P_A)), \quad (3)$$

where the parameter definitions are the same as those in (2) but relate to the parasite. Equations (1–3) are used as the starting point for each of the three analyses described below.

Model Analysis

We take three complementary approaches to analyzing our general model. First, we consider the case of weak selection and fixed genetic variance, which may be appropriate for interactions that generate only weak reciprocal fitness consequences. Next, we relax the assumption of fixed genetic variance by developing a genetically explicit model and applying a QLE approximation (e.g., Nagylaki 1993; Kirkpatrick et al. 2002). This approximation requires selection to be weak on a per locus basis and the rate of recombination to be large relative to the effect of epistasis. Finally, we allow for both the evolution of genetic variance and strong selection by analyzing deterministic numerical simulations of a genetically explicit multilocus model. These three complementary analyses are likely to encompass the range of conditions observed in naturally occurring interspecific interactions.

FIXED GENETIC VARIANCE AND WEAK SELECTION

We begin our analysis by assuming fixed genetic variances for the traits (z_H, z_P) mediating the coevolutionary interaction, weak stabilizing selection (γ_H and γ_P are of order ε), and weak coevolutionary selection (α is of order ε as well). Thus, weak coevolutionary selection is assumed to arise because the probability of infection (eq. 1) depends only weakly on the phenotypes of the interacting species, not because the fitness consequences of infection or resistance are small. With these assumptions, the change in the trait mean of species i is given by the standard quantitative genetics equation

$$\Delta\bar{z}_i = G_i \frac{1}{\bar{W}_i} \frac{\partial \bar{W}_i}{\partial \bar{z}_i}, \quad (4)$$

where G_i is the additive genetic variance for trait z_i in species i, $\bar{z}_i$ is the population mean trait value for species i, and $\bar{W}_i$ is the population mean fitness of species i (Lande 1976, 1979; Abrams 2001). For the specific scenario considered here, equation (4) yields the following equation for the changes that occur in host and parasite trait means across a single generation:

$$\Delta\bar{z}_i \approx G_i\left[\kappa_i - 2\gamma_i\left(\bar{z}_i - \theta_i\right)\right], \tag{5}$$

where terms of order ε^2 and higher have been ignored, and $\kappa_i = \alpha\xi_i/[2(2-\xi_i)]$ measures the strength of selection for increasing host resistance or parasite infectivity (online supplementary Appendix S1).

Three important conclusions are revealed by the analysis of equation (5). First, for the scenario of weak selection considered here, the equations for evolutionary change in host and parasite trait means become decoupled from the trait mean of the opposing species. Thus, even though we explicitly model a coevolutionary hotspot as defined by Thompson (2005), the two species are not coevolving in the strict sense of reciprocal evolutionary change (sensu Janzen 1980). Intuitively, this result arises because evolutionary dynamics are driven by the fitness gradient, which, with our assumption of weak selection is approximately linear and thus does not depend on phenotypic distance. Second, equation (5) shows the only possible outcome of coevolution is an equilibrium state in which selection for increased infectivity or resistance is balanced by constraints placed on these traits by stabilizing selection:

$$\bar{z}_i^* = \theta_i + \frac{\kappa_i}{2\gamma_i}. \tag{6}$$

At this equilibrium, the trait values of host and parasite are uncorrelated and determined only by the relative strengths of selection exerted by the abiotic environment and selection exerted by interspecific interactions. Consequently, there is no expectation that the traits of interacting species should match— regardless of the level of trait remixing—as suggested by the geographic mosaic theory of coevolution and several previous empirical studies (Thompson 1999b, 2005; Brodie et al. 2002; Zangerl and Berenbaum 2003). Finally, equation (5) demonstrates that with weak selection and fixed genetic variance, coevolutionary interactions mediated by phenotype differences do not exhibit cyclical dynamics.

In addition to providing information on the equilibrium values of traits and the overall dynamics of coevolution, equations (6) and (1) can be used together to determine the expected proportion of the host population that can be successfully infected by the parasite at equilibrium. Specifically, integrating our weak α approximation to (1) over host and parasite phenotype distributions and substituting the equilibrium values for host and parasite trait means given by (6), demonstrates that the expected proportion of infected hosts is

$$\begin{aligned} P_A &\approx \frac{1}{2} + \frac{\alpha}{4}\left[\bar{z}_P^* - \bar{z}_H^*\right] \\ &= \frac{1}{2} + \frac{\alpha}{4}\left[\theta_P + \frac{\kappa_P}{2\gamma_P} - \left(\theta_H + \frac{\kappa_H}{2\gamma_H}\right)\right]. \end{aligned} \tag{7}$$

Equation (7) predicts a greater proportion of the host population will be infected as the host becomes increasingly constrained by stabilizing selection (increasing γ_H; decreasing θ_H) or experiences weaker selection for increased resistance (decreasing κ_H)—perhaps due to decreased parasite virulence. Conversely, equation (7) predicts a lesser proportion of the host population will be infected as the parasite becomes increasingly constrained by stabilizing selection (increasing γ_P; decreasing θ_P) or experiences weaker selection for increased infection ability (decreasing κ_P)—perhaps due to the presence of an alternative host.

EXPLICIT MULTILOCUS GENETICS AND WEAK SELECTION

To extend the results of the previous section to cases in which genetic variances evolve, we analyzed our general model in a genetically explicit multilocus framework. The first step in this extension is to specify a mapping between individual genotypes and the phenotypes mediating the interspecific interaction. For simplicity, we assume an individual's phenotype (z_i) is determined by the additive action of n_i diallelic haploid loci with arbitrary phenotypic effects

$$z_i = \sum_{j=1}^{n_i} b_{i,j} X_{i,j}. \tag{8}$$

In equation (8), $b_{i,j}$ is the phenotypic effect of locus j on trait z_i in species i, and $X_{i,j}$ is an indicator variable that takes value 1 or 0 depending on the allele carried by an individual at locus j (Kirkpatrick et al. 2002).

With the additional assumptions that recombination occurs at rate r_i in species i and that mutation is absent, equations (1–3, 8) provide a sufficient basis for generating exact expressions for the changes in genotype frequencies occurring over the course of a single generation. These exact expressions are too complicated to analyze mathematically for all but the simplest cases of one or two genetic loci. For this reason, we make the additional assumption that recombination is quite frequent relative to the per locus strength of selection, allowing us to use a QLE approximation (Kimura 1965; Nagylaki 1993; Kirkpatrick et al. 2002). Under the QLE assumptions of weak selection and frequent recombination, the change in allele frequency that occurs in locus j of species i is given by

$$\Delta p_{i,j} = b_{i,j} p_{i,j} q_{i,j} \times \left(\kappa_i - \gamma_i \left(2 \left(\sum_{j=1}^{n_i} b_{i,j} p_{i,j} - \theta_i \right) + b_{i,j} \left(1 - 2 p_{i,j} \right) \right) \right), \quad (9)$$

where $p_{i,j}$ is the frequency of the "1" allele at locus j in species i (online Appendix 2). Equation (9) can also be derived by simply assuming that linkage disequilibria are absent (e.g., Kopp and Gavrilets 2006).

Analysis of equation (9) reveals several important points. First, as is the case for the model with fixed genetic variance, evolutionary change in the host and parasite is decoupled. This decoupling arises because, here too, we assume the probability of a successful parasite attack varies only weakly across the range of possible host and parasite phenotypes. Second, equation (9) shows that, as long as all loci have equal phenotypic effects ($b_{i,j} = b_i$ for all j), the ultimate outcome of coevolution depends on the magnitude of selection for increasing host resistance or parasite infectivity (κ) relative to stabilizing selection imposed by the abiotic environment (γ). If coevolutionary selection is sufficiently strong to completely overwhelm constraints placed on the trait by stabilizing selection ($\kappa_i/(2\gamma_i) + \theta_i > b_i(n_i - 1/2)$) the resistance/infectivity trait escalates to its maximum value. In contrast, if constraints placed on the trait by the abiotic environment swamp coevolutionary selection for increased resistance/infectivity ($\kappa_i/(2\gamma_i) + \theta_i < b_i/2$) the resistance/infectivity trait will evolve to its minimal value. If coevolutionary selection and abiotic constraints are not too disparate in strength such that neither of the above conditions holds, intermediate levels of the resistance/infectivity trait can be reached. Specifically, if $b_i\,(F + 1/2) > \theta_i + \kappa_i/(2\gamma_i) > b_i\,(F - 1/2)$ then F loci will be fixed for the "1" allele, yielding an intermediate resistance/infectivity trait value of b_iF. In all of these three cases, allele frequencies will approach either zero or one at all loci such that no genetic variation will be present in either species at equilibrium (online supplementary Appendix S3; Zhivotovsky and Gavrilets 1992). Finally, equation (9) predicts cyclical dynamics driven by host–parasite coevolution are impossible, demonstrating that this result—also derived for the model of fixed genetic variance—is quite general when reciprocal selection is weak (online supplementary Appendix S3).

EXPLICIT MULTILOCUS GENETICS AND STRONG SELECTION

Because interactions between parasites and hosts may lead to strong reciprocal selection on the interacting species (Thompson 1998, 1999a; Bishop et al. 2000; Tiffin et al. 2004), we extended our analysis to these cases using deterministic multilocus simulations. These simulations incorporate the exact fitness equations (1–3) into a deterministic multilocus framework and thus do not make any assumptions regarding the magnitude of the model parameters. Our goal was to evaluate whether the results of the previous sections are robust to violations of our assumption regarding weak coevolutionary selection.

Our simulations included the following assumptions not made in our analytical analyses. First, simulations incorporated reversible mutation at a rate of 5×10^{-6} per locus. Second, simulations considered only the case in which the phenotypic effects of all loci were equal to $1/n_i$; this assumption confines the host and parasite trait values to the interval [0,1]. Finally, simulations assumed the optimal value for host and parasite traits was equal to zero, as would be the case if producing any nonzero value of the resistance/infectivity traits required metabolic expenditures and thus imposed a fitness cost.

At the beginning of each simulation run initial allele frequencies were randomly drawn from a uniform distribution on [0,1], and other parameters were randomly drawn from uniform distributions on the following intervals: $[0 \leq \alpha \leq 10]$, $[0 \leq \xi_i \leq 1]$, and $[0 \leq \gamma_i \leq 1]$. We considered cases in which host and parasite trait values were determined by two, three, four, and five freely recombining genetic loci. For each simulation run, we evaluated whether cyclical dynamics occurred or whether equilibrium was reached. Cycling was defined as a change in the direction of trait mean evolution in both species at least three times between generations 2000 and 5000. An equilibrium was considered to have been reached if the sum of the magnitude of change in the trait mean was less than 0.01 across the final 3000 simulation generations for both species (which equates to a per generation rate of change in the population mean equal to 3.33×10^{-6}). Simulations that could not be categorized as either cyclical or equilibrium dynamics (4.28%) were excluded from our analyses. Excluded cases were generally characterized by very weak selection, which prevented a steady state from being reached over the time frame of the simulations. Detailed inspection of individual simulation runs verified the accuracy and validity of these assignments. In addition to determining whether cycles occurred, simulations recorded information on trait means and variances and the proportion of the host population infected by the parasite in the final generation. For each number of host and parasite loci (2, 3, 4, or 5), we ran 20,000 individual simulations, each with randomly selected parameters and initial conditions. Simulation code (C++) and raw simulation data (Microsoft Excel) are available upon request.

Simulations revealed that not only do cyclical dynamics occur, but that they occur with moderate frequency (17.0%), a result not anticipated based upon our analytical approximations. To evaluate the conditions that favor cyclical dynamics, and to shed further light on possible reasons for the discrepancy between our analytical and simulation results, we performed a multivariate

Table 1. Logistic regression coefficients, standard errors, and associated *P* values explaining the probability of cyclical dynamics. Logistic regression was performed on the 76,575 simulation runs, which could be clearly classified as cyclical or equilibrium with all predictor variables coded as continuous with the exception of the number of loci, which was coded as ordinal. The terms *n*[5–4], *n*[4–3], and *n*[3–2] indicate the effect of increasing the number of loci from 4 to 5, 3 to 4, and 2 to 3, respectively.

Term	Estimate	SE	Chi square	Prob>Chi square
Intercept	4.926194	0.154705	1013.9	<0.0001
n[3–2]	0.88018	0.047384	345.05	<0.0001
n[4–3]	−0.10954	0.042164	6.75	0.0094
n[5–4]	−0.16919	0.045317	13.94	0.0002
ξ_P	3.70674	0.126232	862.27	<0.0001
n [3–2]×ξ_P	−2.46988	0.144459	292.32	<0.0001
n [4–3]×ξ_P	−0.81258	0.129954	39.1	<0.0001
n [5–4]×ξ_P	−0.06751	0.135009	0.25	0.6170
ξ_H	3.63828	0.126829	822.91	<0.0001
n [3–2]×ξ_H	−2.54195	0.145662	304.54	<0.0001
n [4–3]×ξ_H	−0.51123	0.129898	15.49	<0.0001
n [5–4]×ξ_H	−0.18557	0.133358	1.94	0.1641
ξ_P×ξ_H	−11.8028	0.235280	2516.5	0.0000
α	0.67065	0.015311	1918.7	0.0000
n [3–2]×α	−0.01184	0.016916	0.49	0.4838
n [4–3]×α	0.03807	0.016070	5.61	0.0178
n [5–4]×α	0.01117	0.016969	0.43	0.5103
ξ_P×α	−0.63177	0.026736	558.39	<0.0001
ξ_H×α	−0.61498	0.026710	530.14	<0.0001
γ_P	−2.74168	0.109426	627.76	<0.0001
n [3–2]×γ_P	2.46284	0.128133	369.44	<0.0001
n [4–3]×γ_P	0.62543	0.117788	28.19	<0.0001
n [5–4]×γ_P	−0.06597	0.122177	0.29	0.5892
ξ_P×γ_P	6.61289	0.196445	1133.2	<0.0001
ξ_H×γ_P	6.68097	0.196303	1158.3	<0.0001
α×γ_P	0.41308	0.023291	314.54	<0.0001
γ_H	−2.76598	0.110740	623.87	<0.0001
n [3–2]×γ_H	2.47097	0.129658	363.2	<0.0001
n [4–3]×γ_H	0.86904	0.119165	53.18	<0.0001
n [5–4]×γ_H	−0.22916	0.122517	3.5	0.0614
ξ_P×γ_H	6.98978	0.198480	1240.2	<0.0001
ξ_H×γ_H	6.72166	0.198645	1145	<0.0001
α×γ_H	0.40027	0.023435	291.72	<0.0001
γ_P×γ_H	−4.76676	0.172945	759.68	<0.0001
ξ_P×ξ_P	−9.28133	0.195678	2249.8	0.0000
ξ_H×ξ_H	−9.56707	0.195017	2406.6	0.0000
α×α	−0.11532	0.002683	1848.3	0.0000
γ_P×γ_P	−4.14626	0.168702	604.05	<0.0001
γ_H×γ_H	−4.27574	0.169196	638.62	<0.0001

logistic regression (JMP 5.01; SAS Institute Inc., Cary, NC) with equilibrium outcomes coded as 0 and cyclical dynamics coded as 1. The parameters α, ξ_i, γ_i, n, and their second-order interactions were used as predictors. This analysis revealed that many parameters had highly significant effects on the likelihood of cyclical dynamics (Table 1). Specifically, the analysis demonstrated that cycles are favored by strong coevolutionary selection (increasing values of α, ξ_H, and ξ_P) and weak stabilizing selection (decreasing values of γ_H and γ_P).

Two other observations can be drawn from our simulation data regarding the values of the selection parameters (α, ξ_i, γ_i) that favor cyclical dynamics. First, although our logistic regression suggests cycles are favored by weak stabilizing selection, in no cases did we observe cyclical dynamics when stabilizing selection was absent altogether, suggesting some minimum threshold of stabilizing selection is required. Second, in no cases did we observe cycles when the value of the parameter α was less than 1.704, which suggests the sensitivity of parasite attack to host and parasite phenotypes must also exceed some critical threshold for cycles to occur. Importantly, this minimum value of the parameter α exceeds that allowed by our analytical approximations, likely explaining why cycles are possible in our simulations but not in our analytical models. This possibility was further confirmed by intensive numerical investigation of several specific cases, by gradually increasing α from low to high values (Fig. 2). In each case we studied, a threshold value of α exists below which cycles do not occur (Fig. 2A, B) but above which cycles do occur (Fig. 2C).

In addition to identifying values of the selection parameters α, ξ_i, and γ_i that promote cyclical dynamics, our logistic regression identified a significant effect of the number of loci as well as numerous significant interactions among parameters (Table 1). For instance, our logistic regression revealed that cycles are most likely when traits are determined by intermediate numbers of loci and when asymmetries exist in the fitness consequences of species interactions (negative interaction between ξ_H and ξ_P) and in the strength of stabilizing selection (negative interaction between γ_H and γ_P) acting on the two species (Table 1). Because cycles are favored by such asymmetries, we expect the topology of the cycles themselves to be asymmetric. Specifically, we expect the species that is less constrained by stabilizing selection and/or more strongly impacted by interspecific interactions to cycle through larger trait values than its opponent. As we will discuss later, these asymmetries greatly reduce the likelihood that trait values of interacting species are positively correlated.

We further analyzed our simulation data to determine whether our analytical prediction that genetic variance would be completely eroded at equilibrium was upheld even when cases of strong selection were considered. For those cases not exhibiting cyclical dynamics, our simulation results strongly support our analytical predictions, with the average genetic variance at generation 5000 being $2.17\times10^{-4} \pm 6.90\times10^{-6}$ SE for the host and $2.10\times10^{-4} \pm 6.50\times10^{-6}$ SE for the parasite, values consistent with a simple balance between mutation and selection. In contrast,

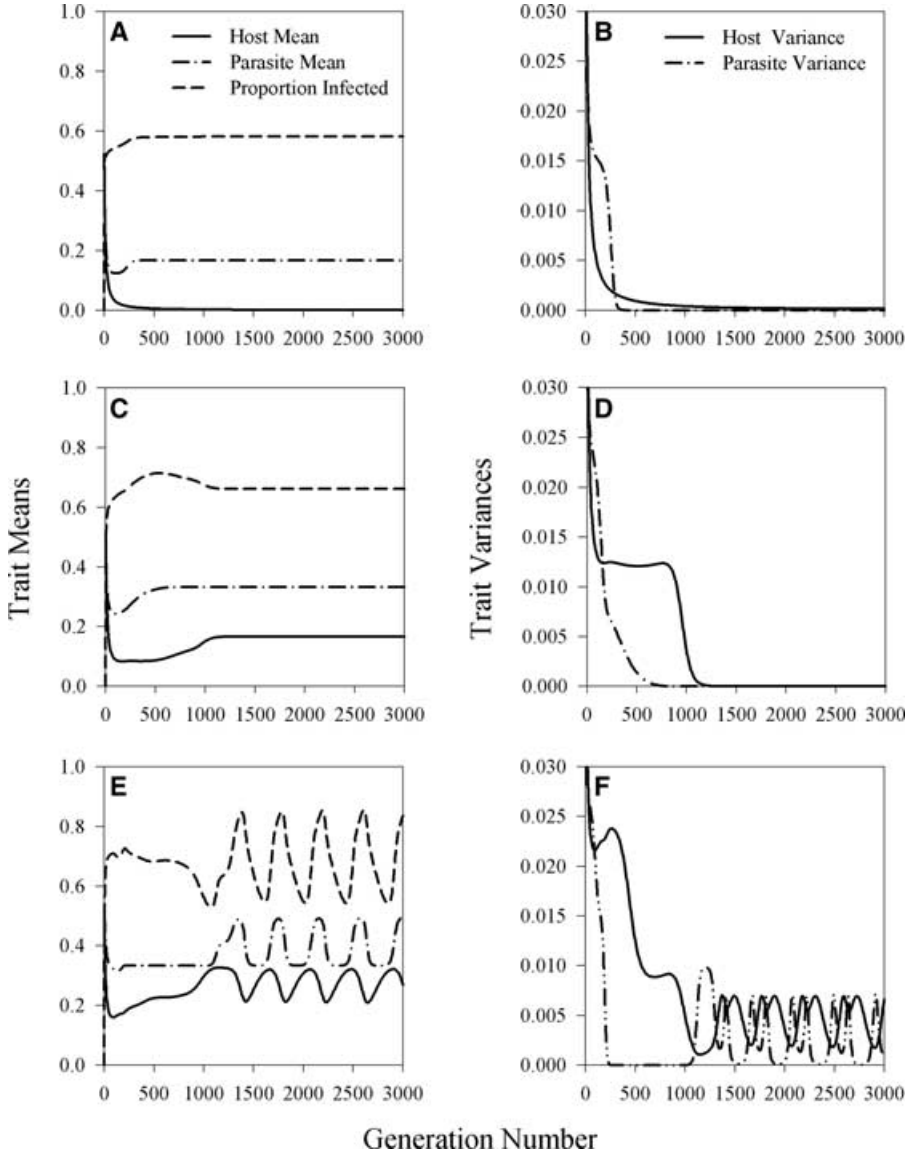

Figure 2. Representative dynamics for trait means and the proportion of the infected hosts (left-hand panels) and genetic variances (right-hand panels) for three different values of α. The value of α was 2.0 in (A) and (B), 4.0 in (C) and (D), and 8.0 in (E) and (F). All other parameters were identical across panels: $\xi_H = 0.3$, $\xi_P = 0.8$, $\gamma_H = 1.1$, $\gamma_P = 1.8$, $n_H = 6$, $n_P = 6$, $r_H = 0.5$, and $r_P = 0.2$.

for those cases in which cyclical dynamics occurred, the average genetic variance at generation 5000 was $1.58\times10^{-2} \pm 1.46\times10^{-4}$ SE for the host and $1.58\times10^{-2} \pm 1.46\times10^{-4}$ SE for the parasite, quantities approximately 70 times larger than noncyclical cases, and significantly larger than the genetic variance expected to be maintained under mutation selection balance alone. Intensive numerical analysis of several specific cases verified these results, showing an absence of genetic variation when α was below the critical threshold value required for cyclical dynamics (Fig. 2). Thus, strong selection in our simulations actually creates the potential for genetic polymorphism to be maintained at significantly greater levels than expected based upon our weak selection approximations.

We also used our simulations to explore the topology of coevolutionary cycles. Specifically, we investigated the average amplitude of coevolutionary cycles as a function of the number of loci. Our results demonstrate that cycles tend to be small in amplitude with amplitude decreasing as the number of loci is increased. This result apparently arises because phenotypic cycles are driven primarily by oscillations at only a single genetic locus. Consequently, the amplitude of phenotypic cycles is expected to be equal to the maximum phenotypic change caused by cycles at a single locus, which, because we confine trait values to the interval [0,1], is equal to $1/n$. This pattern can be clearly seen in Figure 3, which shows the majority of cycles are of amplitude 1/2 inthe case of two loci (Fig. 3B), but 1/4 in the case of four loci

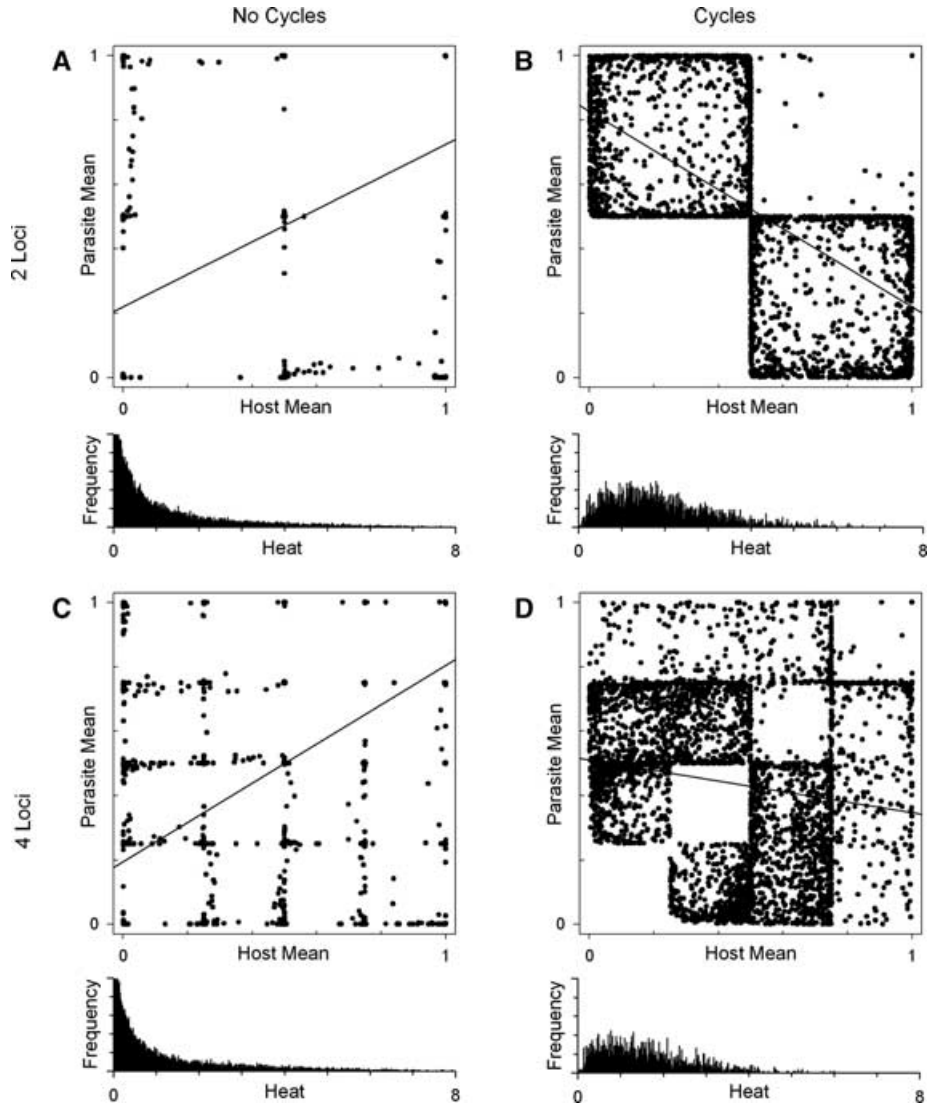

Figure 3. Host population mean phenotypes plotted against parasite population mean phenotypes in generation 5000 of the simulations. Each point represents a single coevolving host–parasite community with parameters and initial allele frequencies selected at random (see text). The solid black lines represent a linear regression of parasite mean phenotype on host mean phenotype. The distribution of the strength of coevolutionary "heat" ($\alpha \times \xi_H \times \xi_P$) is plotted below each scatter plot. (A) shows cases in which phenotypes are determined by two loci and cycles did not occur ($n = 17265$, $R^2 = 0.25499$, $\bar{z}_P = 0.22 + 0.50\bar{z}_H$). (B) shows cases in which phenotypes are determined by two loci and coevolutionary cycles did occur ($n = 2447$, $R^2 = 0.369446$, $\bar{z}_P = 0.83 - 0.61\bar{z}_H$). (C) shows cases in which phenotypes are determined by four loci and cycles did not occur ($n = 15410$, $R^2 = 0.376137$, $\bar{z}_P = 0.19 + 0.61\bar{z}_H$). (D) shows the cases in which phenotypes are determined by four loci and cycles did occur ($n = 3588$, $R^2 = 0.0274132$, $\bar{z}_P = 0.51 - 0.16\bar{z}_H$). Comparing (B) and (D) shows the influence of the number of loci on the amplitude of cycles, with most points in (B) falling on the boundary of cycles with amplitude 1/2, and most points in (D) falling on the boundary of cycles with amplitude 1/4.

(Fig. 3D). An additional consequence of this result is that cycles tend to maintain less genetic variation as the number of loci increase, simply because the single locus that cycles generates a decreasing amount of phenotypic variation.

Analytical results derived under the assumption of weak selection and fixed genetic variance allowed us to predict the proportion of the host population infected by the parasite (see eq. 8). We tested whether this analytical result carried over to our simulations by performing a multiple regression of the infected proportion of hosts on the parameters α, ξ_i, γ_i, n, and their second-order interactions. Prior to this analysis, the proportion of infected hosts was transformed using $y' = \ln(y/(1 - y))$; this transformation corrects for nonnormality of proportions as well as bounding the regression predictions on the desired [0,1] interval. As expected from our analytical results, ξ_H and γ_P had significant negative effects on the proportion of infected hosts, whereas ξ_P and γ_H, had

significant positive effects (Table 2, eq. 7). In contrast, the number of loci ($n_H = n_P = n$), and the sensitivity of the probability of attack to host and parasite phenotypes (α), had no significant effect (Table 2).

Table 2. Multiple regression coefficients, standard errors, and associated *P* values explaining the proportion of the host population infected by the parasite. Multiple regression was performed on the 76575 replicate simulation runs, with all predictor variables coded as continuous with the exception of number of loci, which was coded as ordinal. The terms *n*[5–4], *n*[4–3], and *n*[3–2] indicate the effect of increasing the number of loci from 4 to 5, 3 to 4, and 2 to 3, respectively. For the full model, $R^2 = 0.548$ and $P < 0.00001$.

Term	Estimate	Std Error	*t* Ratio	Prob> |t|
Intercept	−0.0487	0.0293	−1.6600	0.0965
n [3–2]	−0.0142	0.0099	−1.4400	0.1509
n [4–3]	−0.0015	0.0100	−0.1500	0.8774
n [5–4]	0.0009	0.0101	0.0900	0.9271
ξ_P	3.1356	0.0240	130.4900	0.0000
n [3–2]$\times\xi_P$	−0.3978	0.0341	−11.6700	<0.0001
n [4–3]$\times\xi_P$	−0.0469	0.0346	−1.3600	0.1754
n [5–4]$\times\xi_P$	−0.0611	0.0353	−1.7300	0.0834
ξ_H	−3.0959	0.0242	128.1000	0.0000
n [3–2]$\times\xi_H$	0.3858	0.0344	11.2100	<0.0001
n [4–3]$\times\xi_H$	0.0210	0.0346	0.6100	0.5445
n [5–4]$\times\xi_H$	0.0366	0.0349	1.0500	0.2943
$\xi_P\times\xi_H$	0.0336	0.0424	0.7900	0.4289
α	0.0025	0.0024	1.0200	0.3063
n [3–2]$\times\alpha$	−0.0007	0.0034	−0.2100	0.8330
n [4–3]$\times\alpha$	−0.0022	0.0035	−0.6400	0.5228
n [5–4]$\times\alpha$	0.0029	0.0035	0.8200	0.4140
$\xi_P\times\alpha$	0.4739	0.0042	111.5700	0.0000
$\xi_H\times\alpha$	−0.4683	0.0042	110.3000	0.0000
γ_P	−2.1444	0.0241	−89.0600	0.0000
n [3–2]$\times\gamma_P$	0.0127	0.0342	0.3700	0.7113
n [4–3]$\times\gamma_P$	0.0715	0.0347	2.0600	0.0394
n [5–4]$\times\gamma_P$	0.0970	0.0353	2.7500	0.0060
$\xi_P\times\gamma_P$	0.5706	0.0428	13.3400	<0.0001
$\xi_H\times\gamma_P$	1.0307	0.0426	24.1900	<0.0001
$\alpha\times\gamma_P$	−0.2768	0.0043	−65.0400	0.0000
γ_H	2.2241	0.0242	91.7900	0.0000
n [3–2]$\times\gamma_H$	−0.0603	0.0345	−1.7500	0.0803
n [4–3]$\times\gamma_H$	−0.1091	0.0349	−3.1300	0.0018
n [5–4]$\times\gamma_H$	−0.0935	0.0353	−2.6500	0.0081
$\xi_P\times\gamma_H$	−0.9960	0.0427	−23.3200	<0.0001
$\xi_H\times\gamma_H$	−0.5671	0.0429	−13.2300	<0.0001
$\alpha\times\gamma_H$	0.2786	0.0043	64.8900	0.0000
$\gamma_P\times\gamma_H$	−0.0409	0.0429	−0.9500	0.3402
$\xi_P\times\xi_P$	−2.0439	0.0475	−43.0700	0.0000
$\xi_H\times\xi_H$	2.0320	0.0474	42.8700	0.0000
$\alpha\times\alpha$	0.0000	0.0005	0.0200	0.9849
$\gamma_P\times\gamma_P$	2.6665	0.0477	55.9600	0.0000
$\gamma_H\times\gamma_H$	−2.7351	0.0476	−57.4100	0.0000

Next, we used simulation results to examine if there is a tendency for traits of host and parasite to "match" when reciprocal selection is strong. Specifically, we compared the trait means of the host and the parasite in the final generation of our simulations via linear regression (i.e., parasite trait mean vs. host trait mean). In contrast to our analytical prediction, our analysis revealed a statistically significant positive association between host and parasite trait means for those cases that did not cycle ($\bar{z}_P = 0.20 + 0.58\bar{z}_H$; $n = 63562$; $R^2 = 0.337$; Figs. 3A, C). Nevertheless, very few cases were observed where host and parasite traits matched precisely, with the majority of cases deviating significantly from any expectation of literal trait matching (Figs. 3A, C). For cases that cycled our results revealed a somewhat surprising negative association between host and parasite trait means ($\bar{z}_P = 0.59 - 0.29\bar{z}_H$; $n = 13015$; $R^2 = 0.087$; Figs. 3B and D). This negative association arises because cyclical dynamics are favored by interspecific asymmetries in the strengths of the parameters ξ and γ, which also create asymmetries in the extent to which each species can escalate its trait value (Table 1). Consequently, when cycles occur, one species tends to have large trait values (the species with large ξ and small γ) whereas the other tends to have small values (the species with small ξ and large γ).

Because the majority of empirical studies are unlikely to have sufficient time series data available to determine whether cycles are occurring, we also analyzed the extent of trait matching between species across all simulations. This analysis of our pooled simulation data revealed a significant positive association between host and parasite traits ($\bar{z}_P = 0.24 - 0.50\bar{z}_H$; $n = 76575$; $R^2 = 0.25$). Thus, there is an overall tendency for host and parasite traits to match when both cyclical and noncyclical cases are considered simultaneously. To get a better feeling for what empirical studies might actually observe, however, we repeatedly subsampled 20 communities from the pooled simulation data to generate datasets more on par with the scale of experimental studies. Although these smaller samples generally reveal a positive correlation between host and parasite traits, this correlation is highly variable (Fig. 4).

In addition to revealing statistical patterns of trait matching between host and parasite, our simulation data demonstrate that the strength of reciprocal selection (coevolutionary "heat") correlates with the extent to which traits of the interacting species are exaggerated. Specifically, for those cases that do not cycle, coevolutionary "heat"—measured as $\alpha \times \xi_H \times \xi_P$,—explains a significant percentage of the variation (42%) in the extent to which the traits of the interacting species are exaggerated ($\bar{z}_P = 0.27 + 0.17\alpha\xi_H\xi_P$; $n = 63562$; $R^2 = 0.42$; $\bar{z}_H = 0.27 + 0.17\alpha\xi_H\xi_P$; $n = 63652$; $R^2 = 0.42$). For those cases that do cycle, however, only 3% of the variation is explained by coevolutionary "heat" ($\bar{z}_P = 0.38 + 0.04\alpha\xi_H\xi_P$; $n = 13015$; $R^2 = 0.03$; $\bar{z}_H = 0.38 + 0.04\alpha\xi_H\xi_P$; $n = 13015$; $R^2 = 0.02$).

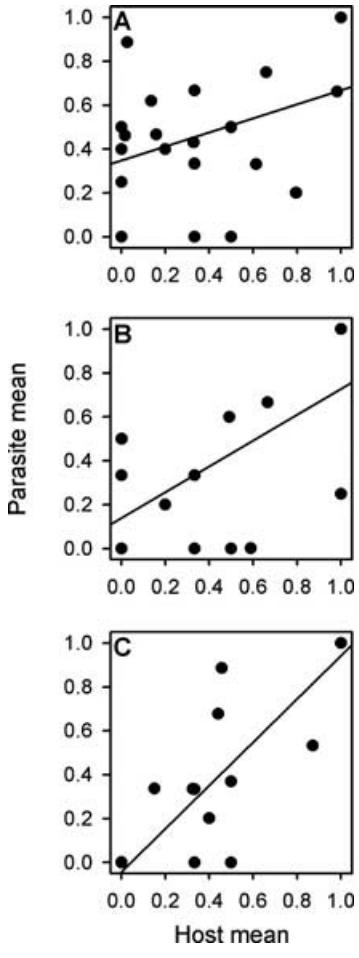

Figure 4. **Parasite population mean phenotypes plotted against host population mean phenotypes for three subsamples of 20 simulated communities drawn at random from the 76575 total simulations. Regression statistics were: (A) $\bar{z}_P = 0.35 + 0.32\bar{z}_H$; $R^2 = 0.14$; (B) $\bar{z}_P = 0.14 + 0.59\bar{z}_H$; $R^2 = 0.35$; (C) $\bar{z}_P = -0.04 + 0.99\bar{z}_H$; $R^2 = 0.72$.**

Discussion

The coevolutionary models analyzed here provide novel predictions for the coevolutionary dynamics and outcomes of interactions mediated by the degree to which the phenotype of one species exceeds that of the other. Such interactions are very common and make up a significant proportion of the most intensively studied cases of coevolution in natural systems (e.g., Berenbaum et al. 1986; Berenbaum and Zangerl 1998; Brodie and Brodie Jr. 1999; Bergelson et al. 2001; Brodie et al. 2002; Toju and Sota 2006). Thus in conjunction with results from previous theory developed for those systems mediated by phenotype matching (e.g., Dieckmann et al. 1995; Abrams and Matsuda 1997; Gavrilets 1997; Nuismer et al. 2005; Kopp and Gavrilets 2006), our results complete a basic sketch of the dynamics and outcomes of coevolutionary interactions mediated by quantitative traits.

An important similarity between results presented here and those reported previously for models of phenotype matching (Dieckmann et al. 1995; Abrams and Matsuda 1997; Gavrilets 1997; Nuismer et al. 2005; Kopp and Gavrilets 2006) is the possibility of cyclical dynamics. Our simulations exhibited cyclical dynamics in 17% of our test cases and predict cycling is particularly likely when small changes in host and parasite phenotypes lead to large changes in the probability of successful parasite attack (i.e., large α). However, our results also highlight important differences between previous models based on phenotype matching and our model based on phenotype excess. Specifically, when interactions are mediated by the extent to which the phenotype of one species exceeds that of the other (i.e., the models studied herein) cyclical dynamics require a minimum strength of coevolutionary selection and the existence of stabilizing selection. In contrast, studies of interactions mediated by phenotype matching have shown that cyclical dynamics can occur in the absence of stabilizing selection and when coevolutionary selection is quite weak (Nuismer et al. 2005). In addition to these differences in the conditions required for cycling, our results show that cyclical dynamics may be of much smaller amplitude in those systems mediated by phenotypic excess than in those systems mediated by phenotype matching. Thus, coevolutionary cycles are likely to occur more frequently, and to be of potentially greater biological significance when coevolution is mediated by phenotype matching rather than phenotype differences, as suggested by Abrams (2000).

In addition to demonstrating that coevolutionary cycles are possible, our results show that phenotypic cycling plays an important role in maintaining genetic variation. Specifically, our simulation results demonstrate that in the absence of coevolutionary cycles, genetic variation cannot be maintained at levels much greater than mutation–selection balance in either host or parasite. In contrast, when selection is strong and cyclical dynamics occur, significantly greater levels of genetic variation can be maintained, particularly when only a small number of loci determine the phenotypes of the interacting species. In both cases, levels of genetic variation are roughly equal in host and parasite. Here too, our results differ in important ways from previous models. Specifically, previous models based on phenotype matching have shown that genetic variation can be maintained even in the absence of cycles and at unequal levels in host and parasite (Nuismer et al. 2005; Kopp and Gavrilets 2006).

These differences arise because of inherent differences in the functional relationship between host and parasite traits and the probability of successful attack in the two types of model (see eq. 1). Models based on phenotype matching lead to selection that is, on average, stabilizing in form for the parasite or predator species, but disruptive in form for the host or prey species (Nuismer et al. 2005). Consequently, genetic variation can often

be effectively maintained in the host species, even in the absence of cyclical dynamics, whereas genetic variation is rapidly eroded in the parasite (Nuismer et al. 2005; Kopp and Gavrilets 2006). Thus, for those coevolutionary interactions mediated by phenotype matching (e.g., Davies and Brooke 1989; Benkman 1999, 2003; Robert and Sorci 1999; Soler et al. 2001; Clayton et al. 2003; Lahti 2005) we expect to see greater levels of genetic variation in the host/prey than in the parasite. However, for those coevolutionary interactions mediated by the extent to which the phenotype of one species exceeds that of the other (Berenbaum and Zangerl 1998; Bergelson et al. 2001; Brodie et al. 2002; Toju and Sota 2006), selection is effectively stabilizing for both interacting species. Thus for these types of interactions we expect genetic variation to be maintained at no more than a single locus and an absence of strong asymmetries in levels of genetic variation across species.

Our results also yield interesting predictions for the expected relationship between host and parasite traits. Specifically, our results reveal that when cyclical dynamics do not occur there should be a positive correlation between host and parasite traits (Figs. 3A, C). In contrast, when cycles do occur, our results reveal a negative correlation between host and parasite traits (Figs. 3B, D). Despite these significant correlations, our results demonstrate that literal matching between host and parasite traits will be very rare, with the majority of interactions showing traits that are dissimilar or "mismatched" to some degree (Figs. 3, 4).

This lack of literal matching between traits has important implications for the interpretation of empirical studies that measure trait values of interacting species in multiple populations (e.g., Berenbaum and Zangerl 1998; Brodie et al. 2002; Toju and Sota 2006). Specifically, our results show that a significant degree of trait mismatching can be explained without invoking gene flow, genetic drift, or extinction/recolonization dynamics (Fig. 4). Consequently, identifying particular populations or geographic regions in which the traits of interacting species do not match does not provide evidence for the geographic mosaic theory (Thompson 1999b, 2005). In conjunction with similar results obtained from models predicated on a mechanism of phenotype matching, our results demonstrate that critical evaluations of the geographic mosaic theory will require studies focused on process rather than pattern (Gomulkiewicz et al. 2007).

ACKNOWLEDGMENTS

We thank S. Gavrilets, R. Gomulkiewicz, M. Servedio, and two anonymous reviewers for helpful comments. This work was supported by NSF grants DEB 0343023 and DMS 0540392 to SLN.

LITERATURE CITED

Abrams, P. A. 2000. The evolution of predator-prey interactions: theory and evidence. Annu. Rev. Ecol. Syst. 31:79–105.

———. 2001. Modelling the adaptive dynamics of traits involved in inter- and intraspecific interactions: an assessment of three methods. Ecol. Letts. 4:166–175.

Abrams, P. A., and H. Matsuda. 1997. Fitness minimization and dynamic instability as a consequence of predator-prey coevolution. Evol. Ecol. 11:1–20.

Benkman, C. W. 1999. The selection mosaic and diversifying coevolution between crossbills and lodgepole pine. Am. Nat. 153:S75–S91.

Benkman, C. W., W. C. Holimon, and J. W. Smith. 2001. The influence of a competitor on the geographic mosaic of coevolution between crossbills and lodgepole pine. Evolution 55:282–294.

Benkman, C. W., T. L. Parchman, A. Favis, and A. M. Siepielski. 2003. Reciprocal selection causes a coevolutionary arms race between crossbills and lodgepole pine. Am. Nat. 162:182–194.

Berenbaum, M. R., and A. R. Zangerl. 1992. Genetics of physiological and behavioral resistance to host furanocoumarins in the parsnip webworm. Evolution 46:1373–1384.

———. 1998. Chemical phenotype matching between a plant and its insect herbivore. Proc. Natl. Acad. Sci. USA 95:13743–13748.

Berenbaum, M. R., A. R. Zangerl, and J. K. Nitao. 1986. Constraints on chemical coevolution: wild parsnips and the parsnip webworm. Evolution 40:1215–1228.

Bergelson, J., G. Dwyer, and J. J. Emerson. 2001. Models and data on plant-enemy coevolution. Annu. Rev. Genet. 35:469–499.

Bishop, J. G., A. M. Dean, and T. Mitchell-Olds. 2000. Rapid evolution in plant chitinases: molecular targets of selection in plant-pathogen coevolution. Proc. Natl. Acad. Sci. USA 97:5322–5327.

Brodie, E. D., and E. D. Brodie Jr. 1999. Costs of exploiting poisonous prey: evolutionary trade-offs in a predator-prey arms race. Evolution 53:626–631.

Brodie, E. D., and B. J. Ridenhour. 2003. Reciprocal selection at the phenotypic interface of coevolution. Integr. Comp. Biol. 43:408–418.

Brodie, E. D., B. J. Ridenhour, and E. D. Brodie. 2002. The evolutionary response of predators to dangerous prey: hotspots and coldspots in the geographic mosaic of coevolution between garter snakes and newts. Evolution 56:2067–2082.

Burdon, J. J., and P. H. Thrall. 1999. Spatial and temporal patterns in coevolving plant and pathogen associations. Am. Nat. 153:S15–S33.

———. 2000. Coevolution at multiple spatial scales: *Linum marginale-Melampsora lini*—from the individual to the species. Evol. Ecol. 14:261–281.

Clayton, D. H., S. E. Bush, B. M. Goates, and K. P. Johnson. 2003. Host defense reinforces host-parasite cospeciation. Proc. Natl. Acad. Sci. USA 100:15694–15699.

Davies, N. B., and M. D. Brooke. 1989. An experimental-study of co-evolution between the Cuckoo, *Cuculus-Canorus*, and its hosts. 1. Host egg discrimination. J. Anim. Ecol. 58:207–224.

Dieckmann, U., P. Marrow, and R. Law. 1995. Evolutionary cycling in predator-prey interactions: population dynamics and the red queen. J. Theo. Biol. 176:91–102.

Fellowes, M. D. E., A. R. Kraaijeveld, and H. C. J. Godfray. 1998. Trade-off associated with selection for increased ability to resist parasitoid attack in *Drosophila melanogaster*. Proc. R. Soc. Lond. B. 265:1553–1558.

Gavrilets, S. 1997. Coevolutionary chase in exploiter-victim systems with polygenic characters. J. Theor. Biol. 186:527–534.

Geffeney, S. L., E. Fujimoto, E. D. Brodie, and P. C. Ruben. 2005. Evolutionary diversification of TTX-resistant sodium channels in a predator-prey interaction. Nature 434:759–763.

Gomulkiewicz, R., D. M. Drown, M. E. Dybdahl, W. Godsoe, S. L. Nuismer, K. M. Pepin, B. J. Ridenhour, C. I. Smith, and J. B. Yoder. 2007. Dos and

don'ts of testing the geographic mosaic theory of coevolution. Heredity *In press*.

Janzen, D. H. 1980. When is it coevolution? Evolution 34:611–612.

Kimura, M. 1965. Attainment of quasilinkage equilibrium when gene frequencies are changing by natural selection. Genetics 52:875–890.

Kirkpatrick, M., T. Johnson, and N. Barton. 2002. General models of multilocus evolution. Genetics 161:1727–1750.

Kopp, M., and S. Gavrilets. 2006. Multilocus genetics and the coevolution of quantitative traits. Evolution 60:1321–1336.

Lahti, D. C. 2005. Evolution of bird eggs in the absence of cuckoo parasitism. Proc. Natl. Acad. Sci. USA 102:18057–18062.

Lande, R. 1976. Natural selection and random genetic drift in phenotypic evolution. Evolution 30:314–334.

———. 1979. Quantitative genetic analysis of multivariate evolution, applied to brain:body size allometry. Evolution 33:402–416.

Nagylaki, T. J. 1993. The evolution of multilocus systems under weak selection. Genetics 134:627–647.

Nuismer, S. L., M. Doebeli, and D. Browning. 2005. The coevolutionary dynamics of antagonistic interactions mediated by quantitative traits with evolving variances. Evolution 59:2073–2082.

Nuismer, S. L., and M. Kirkpatrick. 2003. Gene flow and the coevolution of parasite range. Evolution 57:746–754.

Robert, M., and G. Sorci. 1999. Rapid increase of host defence against brood parasites in a recently parasitized area: the case of village weavers in Hispaniola. Proc. R. Soc. Lond. B Biol. Sci. 266:941–946.

Saloniemi, I. 1993. A coevolutionary predator-prey model with quantitative characters. Am. Nat. 141:880–896.

Soler, J. J., J. M. Aviles, M. Soler, and A. P. Moller. 2003. Evolution of host egg mimicry in a brood parasite, the great spotted cuckoo. Biol. J. Linn. Soc. 79:551–563.

Soler, J. J., J. G. Martinez, M. Soler, and A. P. Moller. 1999. Genetic and geographic variation in rejection behavior of cuckoo eggs by European magpie populations: an experimental test of rejecter-gene flow. Evolution 53:947–956.

———. 2001. Coevolutionary interactions in a host-parasite system. Ecol. Letts. 4:470–476.

Thompson, J. N. 1998. Rapid evolution as an ecological process. Trends Ecol. Evol. 13:329–332.

———. 1999a. The evolution of species interactions. Science 284:2116–2118.

———. 1999b. Specific hypotheses on the geographic mosaic of coevolution. Am. Nat. 153:S1–S14.

———. 2005. The geographic mosaic of coevolution. Univ. of Chicago Press, Chicago.

Tiffin, P., R. Hacker, and B. S. Gaut. 2004. Population genetic evidence for rapid changes in intraspecific diversity and allelic cycling of a specialist defense gene in Zea. Genetics 168:425–434.

Toju, H., and T. Sota. 2006. Imbalance of predator and prey armament: geographic clines in phenotypic interface and natural selection. Am. Nat. 167:105–117.

Webster, J. P., and M. E. J. Woolhouse. 1999. Cost of resistance: relationship between reduced fertility and increased resistance in a snail-schistosome host-parasite system. Proc. R. Soc. Lond. B 266:391–396.

Zangerl, A. R., and M. R. Berenbaum. 2003. Phenotype matching in wild parsnip and parsnip webworms: causes and consequences. Evolution 57:806–815.

Zhivotovsky, L. A., and S. Gavrilets. 1992. Quantitative variability and multilocus polymorphism under epistatic selection. Theor. Pop. Biol. 42:254–283.

Associate Editor: M. Servedio

Supplementary Material

The following supplementary material is available for this article:

Appendix S1. Derivation of Dynamical Equations for the Case of Weak Selection and Fixed Genetic Variance.

Appendix S2. Derivation of Dynamical Equations for the Case of Weak Selection, Frequent Recombination, and Explicit Multi-locus Genetics.

Appendix S3. QLE Analysis of the Multi-locus Model.

This material is available as part of the online article from:
http://www.blackwell-synergy.com/doi/abs/10.1111/j.1558-5646.2007.00158.x
(This link will take you to the article abstract.)

Please note: Blackwell Publishing is not responsible for the content or functionality of any supplementary materials supplied by the authors. Any queries (other than missing material) should be directed to the corresponding author for the article.